

Dynamic Stabilization of Expressed Proteins in Engineered Diatom Biosilica Matrices

Yijia Xiong,[†] Nicole R. Ford,[‡] Karen A. Hecht,[‡] Guritno Roesijadi,^{‡,§} and Thomas C. Squier^{*,†}

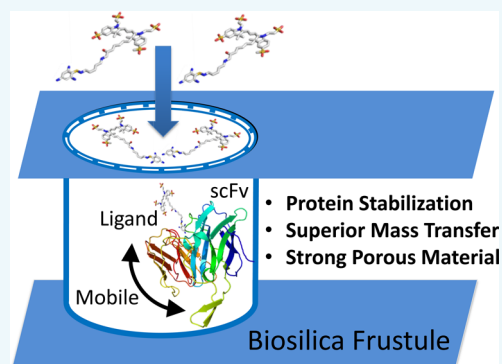
[‡]Marine Biotechnology Group, Pacific Northwest National Laboratory, Sequim, Washington 98382, United States

[§]Department of Microbiology, Oregon State University, Corvallis, Oregon 97331, United States

[†]Department of Basic Medical Sciences, Western University of Health Sciences, Lebanon, Oregon 97355, United States

S Supporting Information

ABSTRACT: Self-assembly of recombinant proteins within the biosilica of living diatoms represents a means to construct functional materials in a reproducible and scalable manner that will enable applications that harness the inherent specificities of proteins to sense and respond to environmental cues. Here we describe the use of a silaffin-derived lysine-rich 39-amino-acid targeting sequence (Sil_{3-T8}) that directs a single chain fragment variable (scFv) antibody or an enhanced green fluorescent protein (EGFP) to assemble within the biosilica frustule, resulting in abundance of >200 000 proteins per frustule. Using either a fluorescent ligand bound to the scFv or the intrinsic fluorescence of EGFP, we monitored protein conformational dynamics, accessibility to external quenchers, binding affinity, and conformational stability. Like proteins in solution, proteins within isolated frustules undergo isotropic rotational motion, but with 2-fold increases in rotational correlation times that are indicative of weak macromolecular associations within the biosilica. Solvent accessibilities and high-affinity (pM) binding are comparable to those in solution. In contrast to solution conditions, scFv antibodies within the biosilica matrix retain their binding affinity in the presence of chaotropic agents (i.e., 8 M urea). Together, these results argue that dramatic increases in protein conformational stability within the biosilica matrices arise through molecular crowding, acting to retain native protein folds and associated functionality with the potential to allow the utility of engineered proteins under a range of harsh environmental conditions associated with environmental sensing and industrial catalytic transformations.



Synthetic biology offers a means to develop cellular factories that allow the low-cost synthesis of chemicals and designer materials (see “A New Biology for the Twenty-first Century”).¹ Examples of these approaches currently involve well-studied organisms, including *E. coli* and *S. cerevisiae*, whose genetics facilitate the introduction of genes encoding proteins within entire synthetic pathways that permit the generation of industrial quantities of precursor chemicals (e.g., 1,3-propanediol) or low-cost pharmaceuticals (e.g., artemisin).² Additional advances are needed to create materials that permit “cell-free” bioprocessing that might include, for example, the cell walls (frustules) of diatoms, as biosilica materials functionally stabilize many bioorganic macromolecules.^{3,4} Along these lines, prior measurements have demonstrated an ability to target specific proteins within living diatoms to organelles linked to biosilica formation, resulting in the creation of highly porous biosilica structures with 18 ± 3 nm spherical nanopores containing embedded proteins capable of mediating analyte binding and catalytic transformation.^{5–8} Such functionalized materials are mechanically strong and potentially useful for a range of existing industrial applications, including those that already use diatomite, in filtration, toothpaste, insecticides, as an absorbent in liquids, and as an activator of blood clotting.²

Further, genetically engineered diatom biosilica expressing the highly stable immunoglobulin G binding domain of protein G (GB1) permits the selective binding of cell-targeting antibodies.⁹ However, current applications are limited to the targeting of highly stable proteins to the biosilica matrix, and have not considered the mechanisms whereby the biosilica matrix can alter analyte binding affinity, substrate accessibility, or catalytic activity that may limit the usefulness of these materials. Furthermore, current approaches of protein immobilization in biosilica result in large reductions in (i) rates of analyte binding and (ii) binding affinities.⁷ Such losses in protein function upon immobilization in biosilica may arise from mechanisms similar to those previously observed following protein adsorption onto synthetic silicate surfaces, which can restrict catalytically important domain motions.¹⁰ In this respect, new bioassembly approaches are needed, like those developed in hydrogels, which tether and stabilize proteins within porous materials while maintaining critical domain movements linked to function.¹¹

Received: March 25, 2016

Revised: May 2, 2016

Published: May 3, 2016

To address the possible utility of biosilica-immobilized proteins, we have used the silaffin-derived lysine rich 39-amino-acid sequence (Sil3_{T8}), previously described by Kröger and colleagues, to target enhanced green fluorescent protein (EGFP) or a single chain fragment variable (scFv) antibody¹² to the biosilica matrix of the diatom *Thalassiosira pseudonana*.^{5,13,14} The stability and natural fluorescence of EGFP aid in the quantification of the protein microenvironment. The scFv antibody was chosen as a prototype of a class of reagents routinely used for detection and diagnostics, which commonly involve engineered protein scaffolds that include domain elements of immunoglobulins and engineered single domain proteins.^{15–17} Furthermore, current clinical applications of engineered protein scaffolds use antibody fragments, such as single chain antibodies (scFv), which represent a dominant new approach in the development of antibody-directed therapies.^{15,18} Advantages of the scFv scaffold include rapid selection against target antigens and the ability to obtain large amounts of antibodies using cost-efficient expression systems.¹⁹ However, widespread applications suffer from significant challenges associated with a need to engineer protein stability, while retaining sufficient flexibility within the antigen binding domain to maintain high-affinity binding. Further, engineered protein scaffolds have a tendency to exhibit poor solubility and commonly aggregate in solution.^{20–23}

Facilitating analysis of the function of the scFv,¹² we have coupled Alexa fluorophores to a derivative of the trinitrotoluene ligand (TNT),²⁴ permitting a determination of how protein targeting affects ligand affinity and accessibility. Dynamic structural measurements of highly fluorescent EGFP were used to identify how the biosilica environment may act to restrict protein motions to enable a mechanistic understanding of how the biosilica environment stabilizes protein function. Finally, possible alterations in protein stability were used to quantify whether protein stabilization requires associated reductions in protein dynamics, as previously reported for adsorbed proteins using mesoporous silicate and hydrogel materials.^{10,11}

To understand the utility of engineered frustules as a platform to detect small molecule ligands, we transformed diatoms with a well characterized scFv antibody against TNT linked to the Sil3_{T8} biosilica targeting peptide.^{12,25} The scFv antibody is tethered within the biosilica matrix, as Sil3-directed fusion proteins are (i) retained within the biosilica despite repeated washing and (ii) capable of interacting with large proteins with masses exceeding 120 kDa.²⁶ Binding was assessed using the fluorescent TNT analog TNB-Alexa488 (Figure S1). This fluorescent analog is a trinitrobenzene linked to the Alexa488 chromophore through a cadaverine linkage, as previously described for TNB-Alexa555.²⁶ These measurements take advantage of the known environmental sensitivity of Alexa488, permitting measurements of changes in the fluorescence lifetime (τ) associated with binding.²⁶ We observe a progressive increase in the fluorescence lifetime of TNB-Alexa488 upon addition of increasing amounts of transformed frustules containing scFv antibodies against TNT; in comparison, there is no change in the fluorescence lifetime of TNB-Alexa488 upon addition of wild-type frustules (Figure 1A). There is a corresponding decrease in the rate of rotational dynamics of TNB-Alexa488 in the presence of transformed frustules, with the appearance of an immobilized component with a rotational correlation time (ϕ_{rot}) exceeding 25 ns that is apparent from a rigorous analysis of correlated errors in the

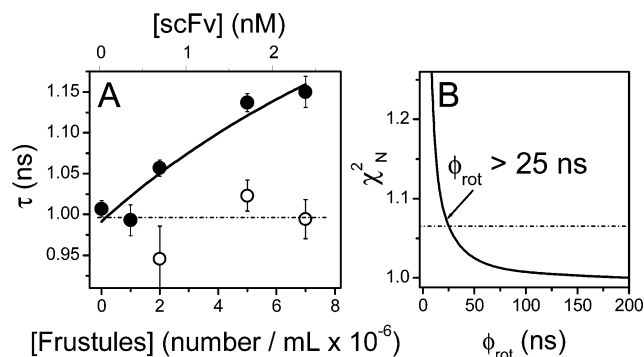


Figure 1. Retention of high-affinity ligand binding for scFv tethered in frustule biosilica. (Panel A) Fluorescence lifetimes (τ) of TNB-Alexa488 (2 nM) in the presence of varying amounts of frustules prepared from wild-type (O) or transformed diatoms expressing scFv antibodies (●). Concentrations of scFv antibody (top axis, panel A) were calculated following determination of maximal binding stoichiometry (see Figure S3). (Panel B) Error surface of normalized χ -squared values for fixed rotational correlation times (ϕ_{rot}) of TNB-Alexa488 (2 nM) bound to scFv in transformed frustules (7.0×10^6 frustules/mL). Horizontal line is the F-statistic for 1 standard deviation. Measurements were made in phosphate buffered saline (PBS) at 25 °C.

fitting parameters (Figure 1B). These results indicate that TNB-Alexa488 binds selectively to the tethered scFv antibodies within the diatom frustule.

To assess whether the scFv antibodies in the transformed diatoms retain a similar high-affinity ligand binding capacity to that observed in solution, we measured the abundance of scFv antibodies present in isolated frustules. This was accomplished through measurements of the fluorescence intensity of bound TNB-Alexa555, which binds with high affinity to this scFv ($K_d = 90$ pM; Figure S2). In the presence of a large excess TNB-Alexa555, less than 0.2% binds to transformed frustules expressing scFv antibodies (Figure S3). These results indicate that there is minimal nonspecific binding between TNB-Alexa555 and the biosilica matrix. Maximal TNB-Alexa555 binding stoichiometries indicate that there are $>200\,000$ scFv antibodies within each transformed frustule. Similar abundances of enhanced green fluorescent protein (EGFP) are apparent when the same Sil3_{T8} targeting peptide is used to express and target EGFP to the biosilica matrix within the diatom frustule,⁵ resulting in $>500\,000$ EGFP in each transformed frustule (Figure S4). These observations indicate that the transformed frustules contain nanomolar concentrations of scFv (6×10^6 frustules/mL = 2 nM scFv) (Figure 1). The observed binding of nanomolar amounts of TNB-Alexa488 (2 nM) upon incubation with transformed frustules expressing nanomolar amounts of scFv antibodies provides strong evidence that the high-affinity binding between TNB-Alexa555 and scFv antibodies observed in solution is retained in transformed biosilica.

The utility of proteins tethered within isolated frustules for environmental monitoring requires that mass transfer (translational diffusion) is not restricted by the biosilica matrix. Using the fluorescence quencher trypan blue (mass = 873 Da), we find that the solvent accessibility is very similar for TNB-Alexa555 bound to scFv_{TNT} ($K_{\text{sv}} = (20 \pm 1) \times 10^4 \text{ M}^{-1}$) and EGFP ($K_{\text{sv}} = (35 \pm 1) \times 10^4 \text{ M}^{-1}$) in transformed frustules, which is expected given the similar fluorescence lifetimes (3.3 ns vs 2.4 ns) and localization patterns (Figure 2). In comparison, quenching efficiencies are lower in solution for

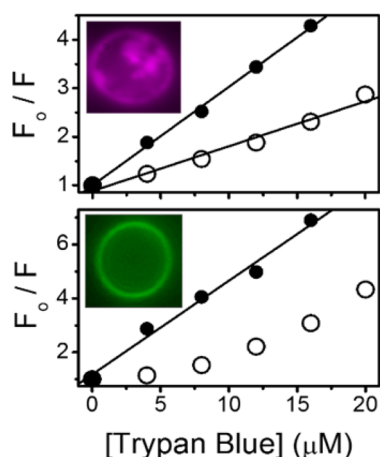


Figure 2. High mass transfer rates in frustule biosilica. Stern–Volmer plots of solvent accessibility for TNB-Alexa555 (Top Panel) or EGFP (Bottom Panel) to quencher trypan blue in solution (12 nM; ○) or for isolated frustule biosilica with TNB-Alexa555 bound to scFv (1.2×10^6 frustules/mL; top) or EGFP (8.8×10^5 frustules/mL; bottom) (●). Insets show images of transformed frustules. Measurements were made in PBS at 25 °C.

unbound TNB-Alexa555 ($K_{sv} = (9.2 \pm 0.1) \times 10^4 \text{ M}^{-1}$) or EGFP ($K_{sv} = (16 \pm 2) \times 10^4 \text{ M}^{-1}$), demonstrating that both proteins within the biosilica matrix remain highly accessible to small molecules. In the case of TNB-Alexa555 bound to scFv within the transformed frustules, the larger K_{sv} in comparison to solution measurements is likely due to the longer fluorescence lifetime that increases the time during which quenching can occur. In contrast, there are no significant differences in the lifetime of EGFP, suggesting that observed differences in quenching efficiencies may be related to the tendency of EGFP to self-associate in solution.²⁷ Irrespective of the physical mechanisms, the very similar quenching efficiencies for both proteins within the biosilica matrix, and their similarity to quenching efficiencies observed in solution, indicates that rates of small molecule mass transfer will not be restricted by the biosilica matrix. These results suggest that the biosilica matrix of isolated frustules offers an environment where binding and catalysis for embedded proteins will not be diffusion limited.

Prior measurements have indicated a functional stabilization of a range of proteins upon their expression within the biosilica frustule.⁶ Understanding the mechanisms associated with protein stabilization is necessary for the routine deployment of proteins for a range of industrial applications. To understand the physical interactions between proteins and the biosilica matrix, we have taken advantage of the superior expression and brightness of EGFP within the biosilica matrix to measure the protein rotational dynamics using frequency-domain fluorescence spectroscopy. Upon increasing the frequency of modulated light, there is an increase in the differential phase and modulated anisotropy, which can be fit using the method of nonlinear least-squares to measure the rotational correlation times associated with protein rotational diffusion (Figure 3). In comparison to EGFP in solution, there is a reduction in the differential phase and modulated anisotropy for EGFP expressed in transformed frustules that is indicative of a reduction in rates of rotational motion. As previously described,²⁸ two rotational correlation times are required to describe the rotational dynamics of EGFP in solution that correspond to a fast ($\phi_1 = 1.1 \text{ ns}$) and a slower rotational

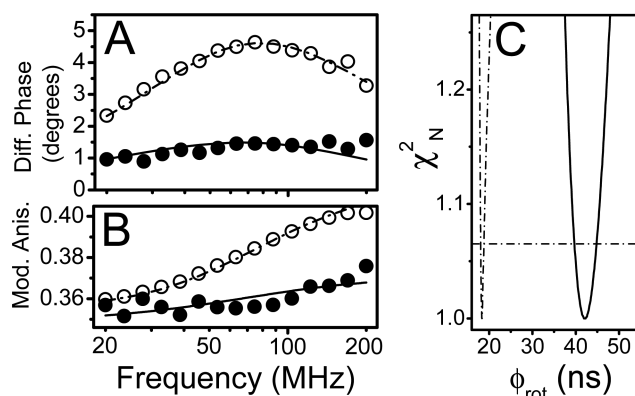


Figure 3. Retention of isotropic rotational dynamics for EGFP within biosilica matrix. Frequency-response of differential phase (Panel A) or modulated anisotropy (Panel B) for EGFP in solution (○) (10 nM) or tethered in biosilica (●) (2×10^6 frustules/mL) with associated nonlinear least-squared fits (lines) for models assuming one (●) or two (○) rotational correlation times (ϕ_{rot}). Normalized χ^2 -squared error surfaces (Panel C) for EGFP in solution (dashed line: $18.3 \pm 0.5 \text{ ns}$) or tethered in biosilica (solid line: $42 \pm 2 \text{ ns}$); horizontal line corresponding to the F-statistic for 1 standard deviation from the mean. Measurements were made in PBS at 25 °C.

correlation time ($\phi_2 = 18.3 \text{ ns}$); the measured rotational correlation time is inversely related to rates of rotational diffusion. The longer rotational correlation time is in close agreement with the calculated rotational correlation time of 15.2 ns based on the crystal structure 4eul.pdb using the program Hydropro²⁹ and prior measurements for the rotational motion of GFP in aqueous buffer of $20 \pm 1 \text{ ns}$.³⁰ In comparison, the rotational dynamics of EGFP within the biosilica matrix can be described with a single rotational correlation time (i.e., $\phi_{rot} = 42 \pm 2 \text{ ns}$) that is very similar to that previously reported for GFP within either the endoplasmic reticulum ($\phi_{rot} = 39 \pm 5 \text{ ns}$) or cytoplasm of cells grown in culture ($\phi_{rot} = 36 \pm 2 \text{ ns}$).³⁰ The large increase in the rotational correlation time for EGFP tethered in biosilica is significant, as there is no overlap in the error surfaces for EGFP in solution and in the biosilica matrix (Figure 3C). The absence of any residual anisotropy in the measurements of the rotational dynamics for EGFP following tethering within the biosilica matrix indicates that EGFP within the biosilica matrix is not adsorbed onto the surface. The approximately 2.5-fold increase in rotational correlation time due to tethering EGFP within the biosilica matrix indicates an increase in the effective viscosity, as there is a linear relationship between GFP rotational dynamics and viscosity.^{30,31} These measurements suggest that immobilized proteins are undergoing unrestricted rotational dynamics, with reductions in overall rotational rates arising from intermolecular interactions that are akin to those observed in living systems.

Reductions in the rotational dynamics of proteins within the biosilica matrix through biomolecular interactions suggest a crowded environment, which may resist protein denaturation. To assess the possible stability of the scFv_{TNT} antibody within the biosilica matrix, we took advantage of the environmental sensitivity of the fluorescence lifetime of TNB-Alexa555. Using frequency-domain fluorescence spectroscopy to measure the fluorescence lifetime, we observe that in comparison to TNB-Alexa555 nonspecifically associated with the biosilica matrix, there is a large shift toward lower frequencies in the frequency response upon binding to the scFv_{TNT} antibody that is

indicative of an increase in the fluorescence lifetime (Figure 4). The increase in the fluorescence lifetime of TNB-Alexa555

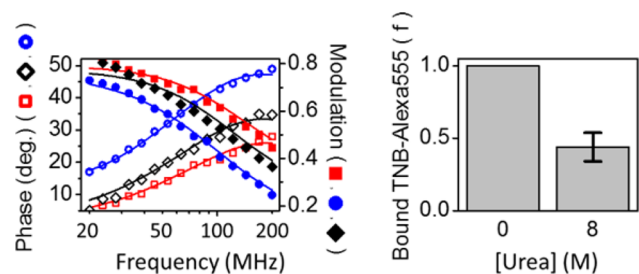


Figure 4. Retention of ligand binding in 8 M urea for scFv tethered in frustule biosilica. (Left Panel) Frequency-domain lifetime data showing increase in phase shift (\square , \diamond , \square) and decrease in modulation (\bullet , \blacklozenge , \blacksquare) upon increasing frequency of modulated light for TNB-Alexa555 bound to wild-type (\square , \blacksquare), or transformed (\circ , \bullet or \diamond , \blacklozenge) frustules (10^6 /mL) before (\circ , \bullet or \square , \blacksquare) or after (\diamond , \blacklozenge) incubation in 8 M urea (2 h). Nonlinear least-squares fits to the data (solid lines) resolve individual lifetimes (τ) for TNB-Alexa555, where $\tau_1 = 3.29$ ns (\circ , \bullet), $\tau_2 = 2.32$ ns (\diamond , \blacklozenge), and $\tau_3 = 1.37$ ns (\square , \blacksquare). All measurements were made in PBS at 25 °C. (Right Panel) Calculated fraction (f) of bound TNB-Alexa555 in the presence of 8 M urea, where $f = (\tau_2 - \tau_3)/(\tau_1 - \tau_3)$.

upon binding the scFv antibody expressed in biosilica is similar to that observed in solution,²⁶ and provides a sensitive means to monitor TNB-Alexa555 binding. Chaotropic agents (i.e., 8 M urea) abolish scFv_{TNT} binding to TNB-Alexa555 in solution (Figure S5), which is consistent with the denaturation of scFv_{TNT}. Under these same denaturing conditions (i.e., 8 M urea), binding is retained between TNB-Alexa555 and scFv_{TNT} within the biosilica matrix, which is apparent from the retention of a significant shift in the frequency response in comparison to unbound TNB-Alexa555 (Figure 4). Analysis of binding using a two-state model suggests that approximately one-half of the scFv_{TNT} retains an ability to bind TNB-Alexa555. A similar stabilization of EGFP is observed following immobilization in biosilica (Figure S6). These results suggest that proteins tethered within the biosilica matrix are stabilized through molecular crowding, and that transformation of diatoms with antibodies represents a path forward toward antibody stabilization that will increase their utility in assays under a range of harsh assay conditions that may, for example, denature antigens to permit their recognition by scFv antibodies within the frustule matrix.

In summary, we have demonstrated that silica-tethered recombinant proteins in diatom frustules are stabilized within a biosilica matrix against chaotropic agents (i.e., 8 M urea) (Figure 4). Silica-tethered recombinant proteins retain the isotropic rotational mobility that is necessary for the retention of high-affinity binding (Figures 1 and 3). Mass transfer is unrestricted through the highly porous biosilica matrix (Figure 2), thereby enabling the use of transformed biosilica for a range of applications involving the detection or chemical transformation of a range of organic molecules, including chemical or biological agents.

■ ASSOCIATED CONTENT

Supporting Information

The Supporting Information is available free of charge on the ACS Publications website at DOI: 10.1021/acs.bioconjchem.6b00165.

Materials and Methods, structures of TNT analogs TNB-Alexa488 and TNB-Alexa555 (Figure S1), TNB-Alexa555 binding affinity to scFv and EGFP (Figure S2), abundances of expressed scFv and EGFP in transformed diatoms (Figures S3 and S4), sensitivity of scFv to denaturation in solution (Figure S5), stability of EGFP in biosilica (Figure S6), and purity of TNB-Alexa488 and TNB-Alexa555 (Figure S7) (PDF)

■ AUTHOR INFORMATION

Corresponding Author

*E-mail: tsquier@westernu.edu.

Notes

The authors declare no competing financial interest.

■ ACKNOWLEDGMENTS

We thank Drs. Nils Kröger and Nicole Poulsen (CUBE Center for Molecular Bioengineering, Dresden, DE) for providing Sil3 clones and Drs. Ellen Goldman and Igor Medintz (Naval Research Laboratory, Washington D.C.) for providing clones for the scFv and assistance in preparing the fluorescent TNT surrogate compounds. This work was supported by the Defense Threat Reduction Agency (G.R. and T.C.S.) and Office of Naval Research (G.R.).

■ REFERENCES

- (1) *A New Biology for the 21st Century* (2009) The National Academies Press, Washington, DC.
- (2) National Research Council of the National Academy; Committee on Industrialization of Biology Industrialization of Biology (2015) *A Roadmap to Accelerate the Advanced Manufacturing of Chemicals*, The National Academies Press, Washington, DC.
- (3) Hudson, S., Cooney, J., and Magner, E. (2008) Proteins in mesoporous silicates. *Angew. Chem., Int. Ed.* 47, 8582–8594.
- (4) Hudson, S., Magner, E., Cooney, J., and Hodnett, B. K. (2005) Methodology for the immobilization of enzymes onto mesoporous materials. *J. Phys. Chem. B* 109, 19496–19506.
- (5) Poulsen, N., Berne, C., Spain, J., and Kröger, N. (2007) Silica immobilization of an enzyme through genetic engineering of the diatom *Thalassiosira pseudonana*. *Angew. Chem., Int. Ed.* 46, 1843–1846.
- (6) Sheppard, V. C., Scheffel, A., Poulsen, N., and Kröger, N. (2012) Live diatom silica immobilization of multimeric and redox-active enzymes. *Appl. Environ. Microbiol.* 78, 211–218.
- (7) Marshall, K. E., Robinson, E. W., Hengel, S. M., Pasa-Tolic, L., and Roesijadi, G. (2012) FRET imaging of diatoms expressing a biosilica-localized ribose sensor. *PLoS One* 7, e33771.
- (8) Hildebrand, M., York, E., Kelz, J. I., Davis, A. K., Frigeri, L. G., Allison, D. P., and Doktycz, M. J. (2006) Nanoscale control of silica morphology and three-dimensional structure during diatom cell wall formation. *J. Mater. Res.* 21, 2689–2698.
- (9) Delalat, B., Sheppard, V. C., Rasi Ghaemi, S., Rao, S., Prestidge, C. A., McPhee, G., Rogers, M. L., Donoghue, J. F., Pillay, V., Johns, T. G., Kröger, N., and Voelcker, N. H. (2015) Targeted drug delivery using genetically engineered diatom biosilica. *Nat. Commun.* 6, 8791.
- (10) Gomes, D. E., Lins, R. D., Pascutti, P. G., Lei, C., and Soares, T. A. (2010) The role of nonbonded interactions in the conformational dynamics of organophosphorous hydrolase adsorbed onto functionalized mesoporous silica surfaces. *J. Phys. Chem. B* 114, 531–540.
- (11) Beech, B. M., Xiong, Y., Boschek, C. B., Baird, C. L., Bigelow, D. J., McAteer, K., and Squier, T. C. (2014) Controlled activation of protein rotational dynamics using smart hydrogel tethering. *J. Am. Chem. Soc.* 136, 13134–13137.
- (12) Liu, J. L., Zabetakis, D., Acevedo-Velez, G., Goldman, E. R., and Anderson, G. P. (2013) Comparison of an antibody and its

recombinant derivative for the detection of the small molecule explosive 2,4,6-trinitrotoluene. *Anal. Chim. Acta* 759, 100–104.

(13) Poulsen, N., and Kroger, N. (2004) Silica morphogenesis by alternative processing of silaffins in the diatom *Thalassiosira pseudonana*. *J. Biol. Chem.* 279, 42993–42999.

(14) Kröger, N., and Brunner, E. (2014) Complex-shaped microbial biominerals for nanotechnology. *Wiley Interdiscip. Rev. Nanomed. Nanobiotechnol.* 6, 615–27.

(15) Nelson, A. L. (2010) Antibody fragments: hope and hype. *mAbs* 2, 77–83.

(16) Skrlec, K., Strukelj, B., and Berlec, A. (2015) Non-immunoglobulin scaffolds: a focus on their targets. *Trends Biotechnol.* 33, 408–418.

(17) Gebauer, M., and Skerra, A. (2009) Engineered protein scaffolds as next-generation antibody therapeutics. *Curr. Opin. Chem. Biol.* 13, 245–255.

(18) de Marco, A. (2011) Biotechnological applications of recombinant single-domain antibody fragments. *Microb. Cell Fact.* 10, 44.

(19) Monnier, P. P., Vigouroux, R. J., and Tassew, N. G. (2013) In vivo applications of single chain Fv (variable domain) (scFv) fragments. *Antibodies* 2, 193–208.

(20) Hugo, N., Lafont, V., Beukes, M., and Altschuh, D. (2002) Functional aspects of co-variant surface charges in an antibody fragment. *Protein Sci.* 11, 2697–2705.

(21) Nichols, P., Li, L., Kumar, S., Buck, P. M., Singh, S. K., Goswami, S., Balthazor, B., Conley, T. R., Sek, D., and Allen, M. J. (2015) Rational design of viscosity reducing mutants of a monoclonal antibody: hydrophobic versus electrostatic inter-molecular interactions. *mAbs* 7, 212–230.

(22) Bradbury, A. (2003) scFvs and beyond. *Drug Discovery Today* 8, 737–739.

(23) Kim, D. Y., Hussack, G., Kandalajt, H., and Tanha, J. (2014) Mutational approaches to improve the biophysical properties of human single-domain antibodies. *Biochim. Biophys. Acta, Proteins Proteomics* 1844, 1983–2001.

(24) Goldman, E. R., Egge, A. L., Medintz, I. L., Lassman, M. E., and Anderson, G. P. (2005) Application of a homogenous assay for the detection of 2,4,6-trinitrotoluene to environmental water samples. *Sci. World J.* 5, 446–451.

(25) Poulsen, N., Scheffel, A., Sheppard, V. C., Chesley, P. M., and Kröger, N. (2013) Pentylsine clusters mediate silica targeting of silaffins in *Thalassiosira pseudonana*. *J. Biol. Chem.* 288, 20100–20109.

(26) Ford, N. R., Hecht, K. A., Hu, D., Orr, G., Xiong, Y., Squier, T. C., Rorrer, G., and Roesijadi, G. (2016) Antigen binding and site-directed labeling of biosilica-immobilized fusion proteins expressed in diatoms. *ACS Synth. Biol.* 5, 193–199.

(27) Krasowska, J., Olasek, M., Bzowska, A., Clark, P. L., and Wielgus-Kutrowska, B. (2010) The comparison of aggregation and folding of enhanced green fluorescent protein (EGFP) by spectroscopic studies. *Spectroscopy* 24, 343–348.

(28) Swaminathan, R., Hoang, C. P., and Verkman, A. S. (1997) Photobleaching recovery and anisotropy decay of green fluorescent protein GFP-S65T in solution and cells: cytoplasmic viscosity probed by green fluorescent protein translational and rotational diffusion. *Biophys. J.* 72, 1900–1907.

(29) Ortega, A., Amoros, D., and Garcia de la Torre, J. (2011) Prediction of hydrodynamic and other solution properties of rigid proteins from atomic- and residue-level models. *Biophys. J.* 101, 892–898.

(30) Dayel, M. J., Hom, E. F., and Verkman, A. S. (1999) Diffusion of green fluorescent protein in the aqueous-phase lumen of endoplasmic reticulum. *Biophys. J.* 76, 2843–2851.

(31) Bertz, A., Ehlers, J. E., Wohl-Bruhn, S., Bunjes, H., Gericke, K. H., and Menzel, H. (2013) Mobility of green fluorescent protein in hydrogel-based drug-delivery systems studied by anisotropy and fluorescence recovery after photobleaching. *Macromol. Biosci.* 13, 215–226.